# Custom-designed nanomaterial libraries for testing metal oxide toxicity

*Suman Pokhrel*[§], *André E. Nel*[ϕ], *Lutz Mädler*[§]

[§]Foundation Institute of Materials Science (IWT), Department of Production Engineering, University of Bremen, Germany

[ϕ]Department of Medicine-Division and California NanoSystems Institute at University of California, Los Angeles, California, USA,

## Supplementary section

### 1. Experimental methods and methodology

***1.1 FSP set up and synthesis of Nanoparticles*:** The flame spray reactor consists of a stainless steel external-mixing nozzle. The liquid precursor is pumped through the inner capillary tube, which projects 0.5 mm above the rest of the nozzle and is dispersed by 5 l/min $O_2$ (pumped through mass flow controllers), which passes through the adjacent annular gap. A standard precursor flow rate of 5 mL/min is supplied to the nozzle by a syringe pump. The annular gap (cross-sectional area of 2.6 $mm^2$ and a corresponding equivalent nozzle diameter of 1.8 mm) is adjusted to a pressure drop of 1 bar across the nozzle tip. The gap (annular gap) is further surrounded by two stainless steel annuli having inner–outer diameters of 9–9.5 and 10–12.5 mm, forming a diffusion flame. The fuel gas ($CH_4$) 1.5 L/min of flows through the inner and supporting gas ($O_2$) 3.2 L/min flows through the outer annulus separately controlled using two mass flow controllers. The reactor also consists of additional sheath with inner–outer diameter of 28–50 mm surrounding the previous outer annulus which can be used for synthesis of materials in different gas atmospheres (in the present study this addition sheath was not used). The particles are formed by reaction, nucleation, surface growth, coagulation and coalescence in the aerosol stream and are collected on glass filters (257 mm diameter) placed at 40 cm above the nozzle after the particles stream are diluted with cold gas. [1, 2]

The metallorganic based precursors such as zinc napthenate (Strem, 99.9% pure) or titanium (IV) isopropoxide (Strem Chemical, 99.9% pure) and Fe napthenate (Strem, 99.9% pure) were used for the synthesis of pure and Fe doped ZnO or $TiO_2$ NPs. All the precursors were dissolved in an organic solvent (xylene, 99.95%, Strem) for spraying. For the synthesis of undoped and Fe-doped ZnO NPs, a 50 mL of zinc naphthenate (0.5 M by metal) was separately mixed with 0-6.5mL of iron naphthenate (0.5 M by metal) to obtain 1-10% of Fe

doping. Similarly, Titanium (IV) isopropoxide (50 mL) was separately mixed with 0-6.5 mL of Fe-napthenate (0.5 M by metal) to make 0-10% of Fe-doped $TiO_2$ nanoparticles.[3, 4]

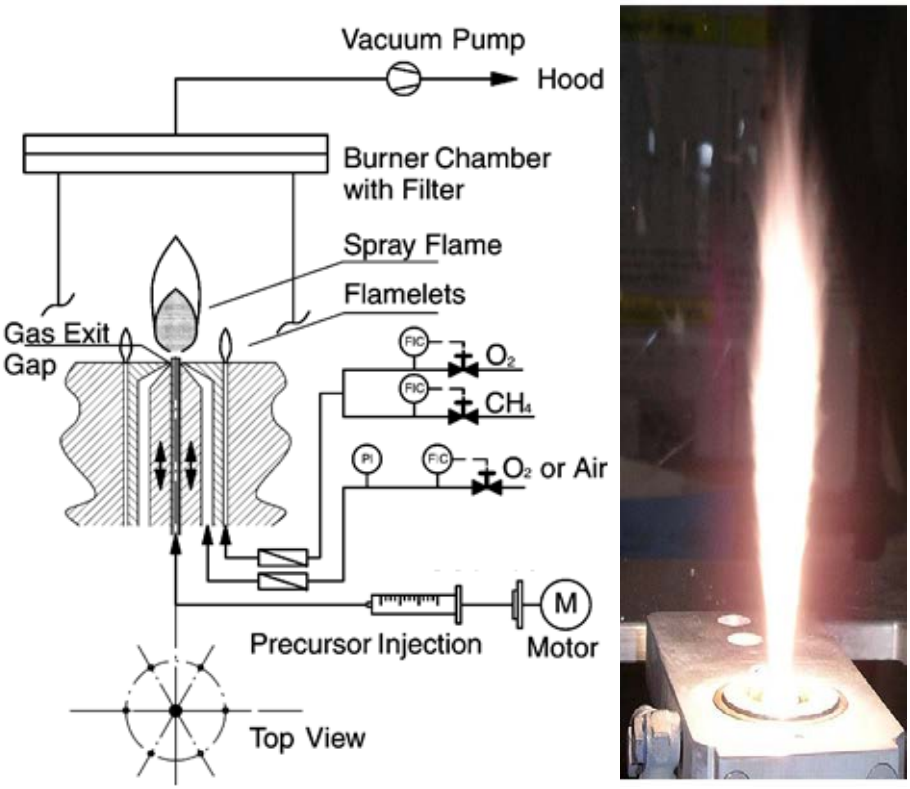


Figure S1. (a) Schematic diagram of the FSP reactor for custom designing[2] the NPs (b) A photograph of a flame during nanoparticle synthesis.

## 2. Characterization of the particles

***2.1 Brunauer-Emmett-Teller (BET), X-ray diffraction (XRD) and TEM analysis of NPs:*** $N_2$ adsorption-desorption measurements were carried out at 77 K using a Quantachrome NOVA 4000e Autosorb gas sorption system. The BET method was used to determine the specific surface areas of the samples. The powders were placed in a test cell and degased for 2 hours at 200°C. X-ray diffraction measurements (XRD) was performed in a reflection mode on the PW 3040/60 X'Pert PRO diffractometer equipped with X'Celerator linear detector using a Cu Kα (λ=0.154 nm) radiation and step size of 0.01°. The microscopic imaging of the specimens were investigated with a FEI Titan 80/300 microscope equipped with a Cs corrector for the objective lens, a Fischione high angle annular dark field detector (HAADF), GATAN post-column imaging filter and a cold field emission gun operated at 300kV as an acceleration voltage (see reference 8 of the revised manuscript for detail).

***2.2 Cellular staining with fluorescent probes and epifluoresence microscopy.*** Two cocktails of fluorescent probe mixtures were prepared by mixing wavelength-compatible fluorescent probes in DMEM media devoid of phenol red. The first cocktail contained Hoechst 33342 (1 μM) and JC1 (1 μM) while the second cocktail contained Hoechst 33342 (1 μM), Fluo-4(5 μM) and propidium iodide (5 μM). The cell-permeable Hoechst 33342 binds to DNA. JC-1 is a cationic dye that accumulates in the mitochondria of healthy cells. Propidium iodide (PI) is a red fluorescent dye that binds to DNA and is excluded from the nucleus of healthy cells by an intact plasma membrane. Fluo-4 is a non-fluorescent cellular dye that is trapped inside living cells and fluoresces green when there is an increase in the cellular [$Ca^{2+}$].[4]

***2.3 Nanoparticle exposure in rats for time dependent toxicity evaluation.*** Tenweek-old C57Bl/6NCrl mice were purchased from Charles River Laboratories (Hollister, CA). Animal exposure to undoped and doped ZnO nanoparticles was carried out by an oropharyngeal aspiration method.[5] Briefly, the mice were anesthetized by intraperitoneal injection of ketamine (100 mg/kg)/xylazine (10 mg/kg) in a total volume of 100 μL. While the animals were held in a vertical position, a 50 μL suspension containing 0.1-20 μg undoped or Fe-doped ZnO nanoparticles was instilled at the back of the tongue to allow pulmonary aspiration. The control animals received the same volume of PBS without particles. Animals were euthanized by injection of 50 mg/kg pentobarbital. One milliliter of saline was used to lavage the lung, with the recovery of 0.8-0.85 mL of BAL fluid. Lung sections were stained with hematoxylin and eosin for assessing neutrophilic inflammation.[5]

***2.4 Pure or Fe doped ZnO dissolution experiments:*** The effect of iron doping on the rate of ZnO dissolution and $Zn^{2+}$ release was studied by adding 6.7-6.9 mg of material to 25 mL of a 0.1 M sodium perchlorate solution at pH 7 and 22°C.[3, 6] The pH was maintained at 7.0±0.4 by adding $HNO_3$ controlled by the pH stat function using auto titrator. The reaction was followed by recording the addition of acid with time and by periodic sampling of 100μL aliquots for total zinc analysis following dilution with 1 mL of electrolyte solution and centrifugation for 5 min at 20000g to remove non-dissolved suspended nanoparticles. A 500μL portion of supernatant was acidified with 500μL of 7% ultra high purity $HNO_3$, and the zinc ion concentration, was measured with ICP-MS.

## 4. Results and discussion

***4.1 Time dependent toxicity evaluation:*** The time dependent *in vivo* results support the relationship observed among biomarkers using Fe-doped ZnO NPs in higher animals.[7] Doses of 37.5, 75, and 150 μg NPs were administered in male rats, which were sacrificed at 1, 14, and 30 days post exposure. The pure ZnO NPs produced a dose-dependent increase in (polymorphonucelar) PMN cell counts in the BAL fluid at 24 h. The respective doses of Fe-doped ZnO caused a significant increase in PMN over controls at all post exposure time while for both undoped and 10% Fe doped particles the influx of PMNs into the lung decreased over a 30 day period. At the highest dose, PMN levels were significantly decreased with Fe doping. Only 10% Fe doped particles were capable of lowering PMN responses to a 150 μg particle dose at the 14 and 30 days. LDH levels in BAL fluid after treatment with Fe-doped ZnO were significantly decreased after 1 and 14 days compared to undoped particles. Albumin levels due to Fe-doped ZnO also decreased significantly after 1, 14, and 30 days treatment compared to undoped particles.

***4.2 Toxicity generation through effective binding:*** NPs bound to proteins in biological fluids constitute an initial nano-bio interface that undergoes dynamic changes when they move into the cells. The kinetics of nanoparticle-protein association-dissociation, and concurrent exchange with free proteins in the media, has important roles in determining the particle's interactions with biological receptors. The channels and receptors shown in Figure 3 in the main text are related to the protein (charged or flexible proteins, catalytic enzymes with sensitive thiol groups, and chelating or interacting proteins) [8, 9] and the metal ion channels through the cell membrane. Ultimately, the massive entry of the ions and the particle uptake in the compartment through these channels causes lysosomal swelling and rupture, leading to particle deposition in the cytoplasm triggering intracellular $Ca^{2+}$ release leading to toxicity. The $Ca^{2+}$ regulated permeability transition pore in mitochondria, potentially leads to decreased ATP production and cellular apoptosis. In addition, the particle uptake into the acidifying endosomal compartment accelerates dissolution.

## References


1. Mädler, L.; Stark, W. J.; Pratsinis, S. E. Rapid synthesis of stable ZnO quantum dots. *J. Appl. Phys.* **2002**, *92*(11), 6537-6540.2.
2. Teoh, W.; Y.; Rose Amal.; Mädler, L.; Flame spray pyrolysis: an enabling technology for nanoparticles design and fabrication, *Nanoscale* **2010**, *2*(8), 1324-1347
3. George, S.; Pokhrel, S.; Xia, T.; Gilbert, B.; Ji, Z. X.; Schowalter, M.; Rosenauer, A.; Damoiseaux, R.; Bradley, K. A.; Mädler, L.; Nel, A. E. Use of a rapid cytotoxicity

screening approach to engineer a safer zinc oxide nanoparticle through iron doping. *ACS Nano* **2010**, *4*(1), 15-29.

4. George, S.; Pokhrel, S.; Ji, Z.; Henderson, B. L.; Xia, T.; Li, L.; Zink, J. I.; Nel, A. E.; Mädler, L. Role of Fe doping in tuning the band gap of $TiO_2$ for the photo-oxidation induced cytotoxicity paradigm. *J. Am. Chem. Soc.* **2011**, *133*(29), 11270-11278.
5. Shvedova, A. A.; Kisin, E.; Murray, A. R.; Johnson, V. J.; Gorelik, O.; Arepalli, S.; 7. Hubbs, A. F.; Mercer, R. R.; Keohavong, P.; Sussman, N.; Jin, J.; Yin, J.; Stone, S.; Chen, B. T.; Deye, G.; Maynard, A.; Castranova, V.; Baron, P. A.; Kagan, V. E. Inhalation vs. aspiration of single-walled carbon nanotubes in C57BL/6 mice: inflammation, fibrosis, oxidative stress and mutagenesis, *Am. J. Physiol. - Lung Cell. Mol. Physiol.* **2008**, *295*, L552.
6. Xia, T.; Kovochich, M.; Liong, M.; Mädler, L.; Gilbert, B.; Shi, H.; Yeh, J. I.; Zink, J. I.; Nel, A. E. Comparison of the mechanism of toxicity of zinc oxide and cerium oxide nanoparticles based on dissolution and oxidative stress properties. *ACS Nano* **2008**, *2*(10), 2121-2134.
7. Xia, T.; Zhao, Y.; Sager, T.; George, S.; Pokhrel, S.; Li, N.; Schoenfeld, D.; Meng, H.; Lin, S.; Wang, X.; Wang, M.; Ji, Z.; Zink, J. I.; Mädler, L.; Castranova, V.; Lin, S.; Nel, A. E. Decreased dissolution of ZnO by iron doping yields nanoparticles with reduced toxicity in the rodent lung and zebrafish embryos. *ACS Nano* **2011**, *5*(2), 1223-1235.
8. Gilbert, B.; Fakra, S. C.; Xia, T.; Pokhrel, S.; Mädler, L.; Nel, A. E. The Fate of ZnO Nanoparticles Administered to Human Bronchial Epithelial Cells *ACS Nano* 2012, *6* (6), 4921-4930.
9. Nel, A. E.; Mädler, L.; Velegol, D.; Xia, T.; Hoek, E. M. V.; Somasundaran, P.; Klaessig, F.; Castranova, V.; Thompson, M. Understanding biophysicochemical interactions at the nano-bio interface. *Nat. Mater.* **2009**, *8*(7), 543-557.